Peer Reviewed

Title:
Potential Inundation Due to Rising Sea Levels in the San Francisco Bay Region

Author:
Knowles, Noah, USGS

Abstract:
An increase in the rate of sea level rise is one of the primary impacts of projected global climate change. To assess potential inundation associated with a continued acceleration of sea level rise, the highest resolution elevation data available were assembled from various sources and mosaicked to cover the land surfaces of the San Francisco Bay region. Next, to quantify extreme water levels throughout the bay,

a hydrodynamic model of the San Francisco Estuary was driven by a projection of hourly water levels at the Presidio. This projection was based on a combination of climate model outputs, an empirical model, and observations, and incorporates astronomical, storm surge, El Niño, and long-term sea level rise influences.

Based on the resulting data, maps of areas vulnerable to inundation were produced, corresponding to specific amounts of sea level rise and recurrence intervals, including tidal datums. These maps portray areas where inundation will likely be an increasing

concern. In the North Bay, wetlands and some developed fill areas are at risk. In Central and South bays, a key feature is the landward periphery of developed areas that would be newly vulnerable to inundation. Nearly all municipalities adjacent to South Bay face

this risk to some degree. For the bay as a whole, as early as mid-century under this scenario, the one-year peak event nearly equals the 100-year peak event in 2000. Maps of vulnerable areas are presented and some implications discussed. Results are available for interactive viewing and download at http://cascade.wr.usgs.gov/data/Task2b-SFBay.

Supporting material:

Figure01_Knowles.tif
Figure02_Knowles.tif
Figure03_Knowles.tif
Figure04_Knowles.tif
Figure05_Knowles.tif
Figure06_Knowles.tif
Figure07_Knowles.tif
Figure08_Knowles.tif
Figure09_Knowles.tif
FigureS1_Knowles.tif

Copyright Information:

SAN FRANCISCO SCIENCE
ESTUARY & WATERSHED

Potential Inundation Due to Rising Sea Levels in the San Francisco Bay Region

Noah Knowles[1], U.S. Geological Survey, Menlo Park, CA 94025

ABSTRACT

An increase in the rate of sea level rise is one of the primary impacts of projected global climate change. To assess potential inundation associated with a continued acceleration of sea level rise, the highest resolution elevation data available were assembled from various sources and mosaicked to cover the land surfaces of the San Francisco Bay region. Next, to quantify extreme water levels throughout the bay, a hydrodynamic model of the San Francisco Estuary was driven by a projection of hourly water levels at the Presidio. This projection was based on a combination of climate model outputs, an empirical model, and observations, and incorporates astronomical, storm surge, El Niño, and long-term sea level rise influences.

Based on the resulting data, maps of areas vulnerable to inundation were produced, corresponding to specific amounts of sea level rise and recurrence intervals, including tidal datums. These maps portray areas where inundation will likely be an increasing concern. In the North Bay, wetlands and some developed fill areas are at risk. In Central and South bays, a key feature is the landward periphery of developed areas that would be newly vulnerable to inundation. Nearly all municipalities adjacent to South Bay face

this risk to some degree. For the bay as a whole, as early as mid-century under this scenario, the one-year peak event nearly equals the 100-year peak event in 2000. Maps of vulnerable areas are presented and some implications discussed. Results are available for interactive viewing and download at *http://cascade.wr.usgs.gov/data/Task2b-SFBay*.

KEYWORDS

Sea level rise, climate change, estuary, San Francisco Bay, flooding, wetlands

INTRODUCTION

An increase in the rate of rise of mean sea level is one of the primary and potentially most troublesome aspects of projected climate change. Sea level at San Francisco's Presidio tide gauge has risen at a rate of 22 centimeters (cm) per century over the last century (Flick 2003), consistent with global average rates (Church and others 2004). In recent years, the rate of global sea level rise increased significantly over that of the previous several decades (Church and White 2006; Bindoff and others 2007). As global temperatures continue to increase, sea level will continue to rise in response, probably at a greater rate than observed historically. While it is generally accepted that global climate warming will increase

1 Corresponding author: *nknowles@usgs.gov*

rates of sea level rise, the range in projected rates is wide, due mainly to the uncertainty in the amount of meltwater from land-based ice in Greenland and Antarctica. Recent projections (Rahmstorf 2007) estimate the range of increase of global sea level by 2100 at 50–140 cm above recent levels. Another recent study (Pfeffer and others 2008) produced a somewhat higher estimate (80–200 cm), reinforcing the opinion that sea level rise during the next several decades could exceed the estimates provided by the Intergovernmental Panel on Climate Change (IPCC) Third and Fourth Assessments (IPCC 2001, 2007). Concerning the high end of the range, Pfeffer and others (2008) concluded that sea level rise is very unlikely to exceed 200 cm by 2100. Beyond 2100, however, sea levels are expected to continue to rise for several centuries due to oceanic thermal inertia (Wigley 2005).

Pioneering studies by Williams (1985, 1987) and Gleick and Maurer (1990) were the first to estimate the impacts of sea level rise in San Francisco Bay. Williams found that a 100-cm sea level rise would result in an inland shift of the estuarine salinity field of 10 to 15 kilometers (km), potentially threatening ecosystems and freshwater supplies. In their comprehensive effort, Gleick and Maurer estimated that a 100-cm sea level rise would result in losses of residential, commercial and industrial structures bordering the bay valued at $48 billion (1990 dollars).

A detailed assessment of what areas adjacent to the bay are vulnerable to inundation due to projected sea level rise is necessary to help avoid future risk in developing residential and commercial areas, to inform infrastructure planning (for example, water treatment outflows and roadways), and to design wetland restoration efforts with the ability to adapt to future changes, among other applications. The present study uses hydrodynamic modeling in conjunction with the most accurate elevation data available to develop high-resolution maps of areas vulnerable to periodic inundation corresponding to varying amounts of sea level rise, and to a range of inundation return intervals. The data are publicly available for use in other efforts at *http://cascade. wr.usgs.gov/data/Task2b-SFBay*.

This study addresses only the question of which areas are vulnerable to inundation, as opposed to quantifying the actual risk of inundation under a future scenario. No distinction is made between vulnerable areas already protected by levees and those that are not—at the time of this study, insufficient data on levees were available to make this distinction. Thus, potential improvements to existing levees or construction of new levees are not considered. Where levees currently exist, the results presented below indicate areas that would be flooded if these levees were to fail (due to, for example, a high-water event or an earthquake). Also, shoreline erosion and the potential accumulation of sediment and organic matter in wetlands are not accounted for here. As levee data become available and as modeling capabilities improve, future studies will address such issues and directly evaluate possible mitigation actions.

In the following sections, the elevation data set and hydrodynamic modeling approach used are described. Then some key results are presented and discussed, including maps and analysis of (1) areas vulnerable to periodic inundation by extreme high-water levels, and (2) wetlands vulnerable to changing tidal datums as sea levels rise. Finally, implications of the results and important caveats are discussed.

## DATA AND METHODS

Method Overview

This study uses a hydrodynamic model to simulate water levels throughout San Francisco Bay under conditions of projected sea level rise. Statistical analysis of the projected water levels provides characterization of both long-term trends in mean sea level and high-water levels associated with short-term variability at points along the bay's shoreline. These high-water levels are then compared to nearby land-surface elevations to determine areas vulnerable to inundation around the bay. The same evaluation is also performed for high and low tidal datums. The focus here is on evaluating specific amounts of sea level rise, which can then be associated with particular future dates according to a given climate scenario, rather than focusing on specific scenarios from the

outset. Where time frames for given amounts of sea level rise to occur are considered, they are based on the range of projections by Rahmstorf (2007).

Elevation Data

To serve as the foundation of this study, the highest resolution elevation data available to date were assembled and mosaicked to cover the entire region. This new data set necessarily represents a patchwork of LiDAR (light detection and ranging) data from multiple sources, photogrammetry data, and IfSAR (interferometric synthetic aperture radar) data where no better data were available. This data set contains elevation data from six sources (Figure 1):

1. FEMA LiDAR, produced by Merrick and Company for use in FEMA's Flood Insurance Rate Maps. These data were processed to a horizontal resolution of 1 m, and the vertical 95% confidence interval is ±30 cm.

2. Sacramento-San Joaquin Delta Region LiDAR data set, produced by the California Department of Water Resources from missions flown in 2007 and 2008. The data set's horizontal resolution is 1 meter (m), and the vertical 95% confidence interval is ±18 cm.

3. Napa watershed LiDAR from the University of California at Berkeley Data Distribution Center for the National Center for Airborne Laser Mapping (NCALM, *http://calm.geo.berkeley.edu/ncalm*). These data are from flights in 2003, the horizontal resolution is 1 m, and the vertical 95% confidence interval is ±30 cm.

4. South Bay salt ponds LiDAR data (Foxgrover and Jaffe 2005). These data are from flights in 2004, and the horizontal resolution is 1 m. The vertical 95% confidence interval is ±25 cm for most of the salt-pond areas, and ±15 cm for the hard, flat surfaces which constitute most of the area vulnerable to future inundation with sea level rise in South Bay.

5. San Francisco region photogrammetric elevation data. The U.S. Geological Survey (USGS), in cooperation with the National Geospatial-Intelligence Agency (NGA), developed ground elevation data

FEMA LiDAR (1m)
DWR LiDAR (1m)
NCALM LiDAR (1m)
Salt Ponds LiDAR (1m)
Photogrammetry (2m)
IfSAR (5m)
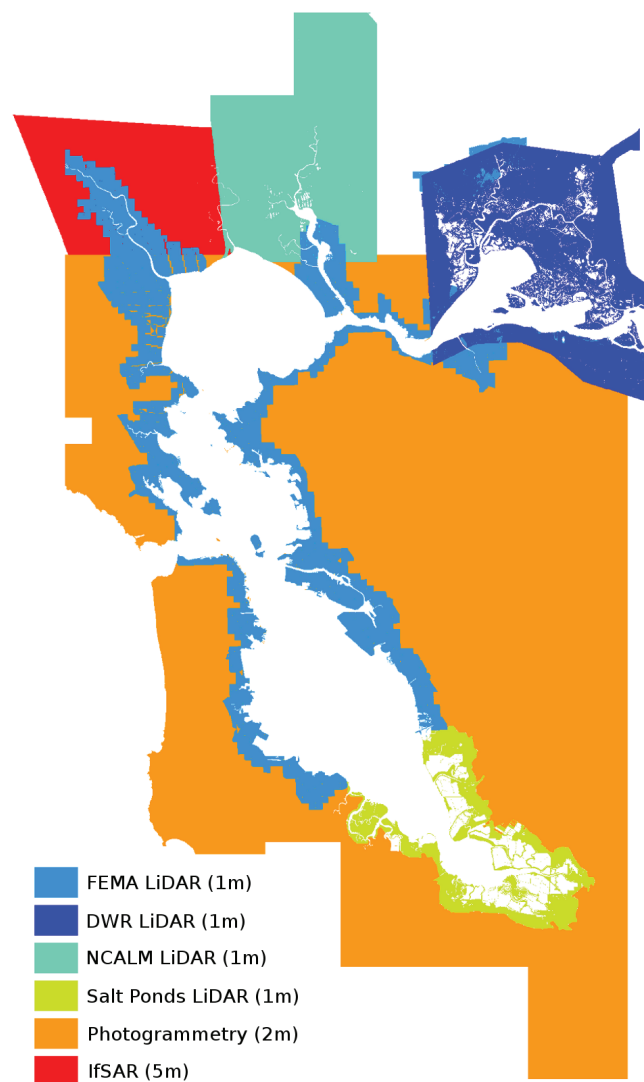
Figure 1 Sources of elevation data. Horizontal resolutions of original data are given in parentheses. All datasets were re-sampled to 2 m and merged.

from flights in 2003 at a horizontal resolution of 2 m for the purpose of producing orthorectified images. We assembled the tiles of elevation data and adjusted them to the North American Vertical Datum of 1988 (NAVD88) datum using the GEOID03 model, resulting in a data set covering the greater bay-delta region (Coons and others 2008). Vertical accuracy was not rigorously determined, but we estimate the 95% confidence interval as ±50 cm.

6. Intermap IfSAR data, produced using synthetic aperture radar methods, were obtained to fill gaps in the Petaluma River and Sonoma Creek watersheds. These data are not ideal, as they have a 5-m horizontal posting and a vertical 95% confidence interval of ±100–200 cm. However, at the time of this writing they are the most accurate data available for the portions of that area not covered by the other data sets.

All elevation data were referenced to NAVD88 in the Universal Transverse Mercator projection (zone 10). Where necessary, the conversion to NAVD88 was made using the GEOID03 model *(http://www.ngs. noaa.gov/PC_PROD/GEOID03)*.

These six data sets were resampled to a common horizontal resolution of 2 m using the nearest-neighbor method, then merged after comparison in areas of overlap. Agreement between all overlapping data sets was good, with slight average positive biases (10–20 cm) of the photogrammetry and IfSAR relative to the LiDAR data sets. This bias makes sense as all of the LiDAR data sets represent "bare-ground" elevations, whereas the photogrammetry and IfSAR data include the height of vegetation. As such, any estimates of inundation vulnerability in areas covered by the photogrammetry and IfSAR data sets may be considered conservative. However, of the six sources used to produce the composite elevation data set, the four LiDAR data sets, all with vertical 95% confidence intervals of less than 30 cm, together constitute 88% (at a minimum—more depending on the amount of sea level rise being evaluated) of the area vulnerable to inundation as presented in this paper.

The last step in developing the regional elevation data set was to mask out open water, as none of the measurement methods described above produce reliable results over water. First, a water mask produced by Foxgrover and Jaffe (2005) for the South Bay LiDAR data based on return characteristics was used to mask open water in the part of the bay covered by that data set. Next, two shoreline data sets representing the mean high water (MHW) tidal datum were used to mask data below this datum throughout the bay. Outside the mouth of San Francisco Bay, the shoreline was extracted from the National Oceanic and Atmospheric Administration (NOAA) National Shoreline data set (*http://shoreline.noaa. gov/data/datasheets*). Inside the bay, another data set was available—a shoreline coverage extracted from the San Francisco Estuary Institute (SFEI) EcoAtlas (*http://www.sfei.org/ecoatlas*). The SFEI and NOAA shoreline data sets were checked against orthoimages from 2003, and it was qualitatively determined that the SFEI shoreline was more accurate. The two shorelines were clipped and joined at the Golden Gate, and used to remove all elevation data below the MHW tidal datum (due to this cutoff, the results discussed below generally exclude mud flats). As of this writing, the resulting composite data set represents the most accurate elevation data publicly available (excluding the IfSAR data which are under a restrictive license) covering the San Francisco Bay region.

Hydrodynamic Model Configuration and Validation

To assess what land elevations around the bay are vulnerable to periodic inundation, estimates of high-water levels throughout the bay must be generated. These high water excursions are the result of tides, storm surge, and other dynamic processes, requiring the use of a hydrodynamic model for this task. This model is used to produce a single 100-year projection of hourly water levels throughout the bay for use in the subsequent analysis. TRIM-2D (Cheng and others 1993) is a numerical model that uses a semi-implicit finite-difference method for solving the two-dimensional shallow water equations in San Francisco Bay. The model uses a 200 m horizontal grid with nearly 50,000 grid cells and is configured here with a six-minute time step. Note that these spatial and temporal resolutions are more than sufficient to capture the highest frequency of water-level variability addressed in this work—semi-diurnal. The model is driven solely by water-level time series at its seaward and landward boundaries, which are translated in phase and amplitude from the tide gauges with sufficiently long records nearest these boundaries, namely the Presidio and Port Chicago stations (Figure 2). Cheng and others (1993) demonstrated that the TRIM-2D hydrodynamic model accurately reproduces the historical amplitudes and phases of tidal constituents throughout the bay.

4
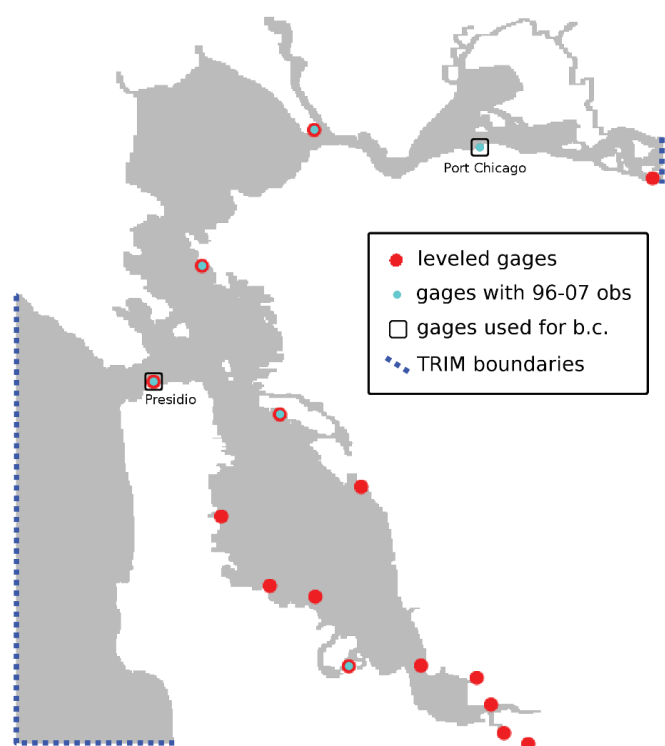
Figure 2 Key sites and features relevant to configuration and validation of TRIM-2D. The model grid is in gray. Gauge sites whose elevation relative to NAVD88 is known are in red. Gauges with data covering the validation period 1996–2007 are in bright blue. The two gauges whose data are used to derive conditions at the model boundaries (dotted blue lines) are in black squares.

The TRIM-2D model was chosen because it is capable of performing the century-long simulation needed to address the effects of long-term climate change in a reasonable amount of time. While the ideal model for this study would have a boundary condition much farther upstream than Port Chicago to avoid boundary issues and would directly simulate the hydrodynamics of inundated areas, such a model is not yet publicly available. Those proprietary models which do include such features are currently too computationally demanding to perform the needed runs in a reasonable amount of time.

The TRIM-2D model in its native configuration simulates water levels relative to mean lower-low water (MLLW), but water levels relative to NAVD88 are needed for comparison with the elevation data. The model takes as input a datum file, which was previ-

ously configured relative to the MLLW tidal datum. By adjusting this file appropriately, the model can be reconfigured to generate output water heights relative to NAVD88. To accomplish this reconfiguration, heights of MLLW relative to NAVD88 from 15 leveled tide gauges throughout the bay (Figure 2) were obtained from NOAA (*http://tidesandcurrents.noaa. gov*). These heights were then interpolated using the method of regular splines with tension (Mitasova and Hofierka 1993) to produce a MLLW adjustment grid. This grid was used in the new input datum file to TRIM-2D, and the resulting simulated water heights are referenced to NAVD88. While NOAA produces a similar datum adjustment grid for the bay region (*http://vdatum.noaa.gov*), the version available at the time of this study was deemed too inaccurate to use, as its source data did not include enough tidal stations in South Bay or near the delta, and spot checks against tidal datums from leveled tide gages revealed inconsistencies.

With the model's datum adjusted, the calibration coefficients used to translate the boundary forcings from the nearby tide gauges to the model boundaries needed to be retuned. To this end, the model was run repeatedly over the period 1996–2007. This validation period was chosen because hourly water-level observations at six sites throughout the bay (Figure 2), including the gauges used to generate the boundary conditions, were available for the full period. The calibration coefficients were iteratively adjusted to minimize differences between simulated and observed mean sea level and average daily tidal range at these six sites.

Hydrodynamic Model Inputs

TRIM-2D requires two time series as inputs—water levels at six-minute intervals at the Presidio and Port Chicago sites—which are then mapped using calibrated coefficients to serve as the model's boundary conditions (Figure 2). A 100-year projection of mean sea level at the Presidio location was produced by Cayan and others (2009) using the method of Rahmstorf (2007), based on global mean temperatures as projected by the CCSM3 global climate model (*http://www.ccsm.ucar.edu*) under the A2 greenhouse

gas emissions scenario (Figure 3). This model projects a ~4.5°C (~8.1°F) increase in global average surface air temperatures by 2100. This is a relatively high (but not the highest) amount of warming among the ensemble of IPCC Fourth Assessment model results (IPCC 2007). Using the Rahmstorf method, this warming corresponds to a 139-cm rise in mean sea level, which corresponds to the upper end of the range of sea level rise projections in his 2007 paper.
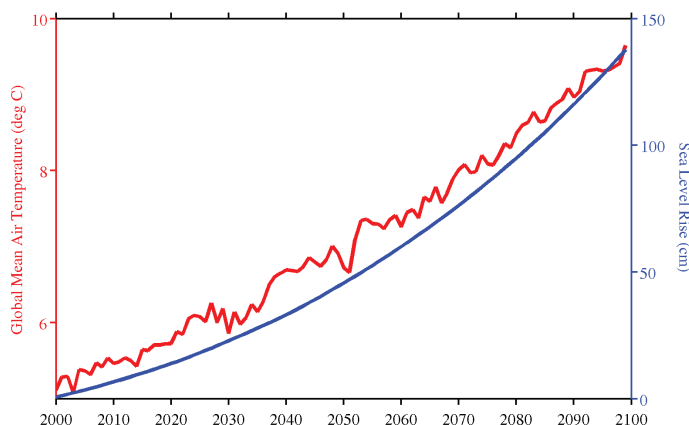
Figure 3 Annual global mean surface air temperatures (red) from the CCSM3-A2 GCM output, and corresponding relative sea level rise (blue) from the Rahmstorf model

This method provided the secular trend in water levels at the Presidio, but water levels vary under the influence of several forces over multiple time scales. Astronomical tides, storm surges, storm-related pressure drops, and El Niños are all major contributors to water-level variability. The result of these and other forces is that water levels reach successively higher peak water levels at longer time scales. Figure 4 illustrates the historical (1900–2000) average daily, monthly, and yearly high-water levels compared to hourly data for a typical year (2006) at the Presidio.

To incorporate this variability into the projected water-level time series, historical variability was superposed on the projected long-term trend in mean sea level. To do this, hourly water-level data (1900–1999) from the Presidio gauge were detrended using a least-squares linear fit to remove any historical sea level rise signal. A few small gaps in the historical data were filled using hindcast astronomical tides
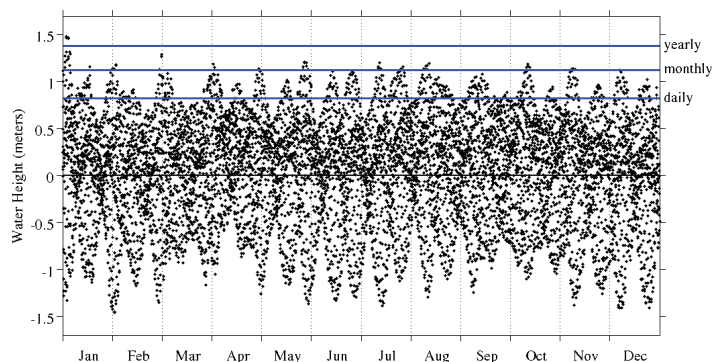
Figure 4 Hourly water levels at the Presidio for a typical year (2006), showing average historical (1900–2000) daily, monthly, and yearly high water levels

(Cheng and Gartner 1984). The resulting 100-year detrended time series, which contained variability over periods ranging from tidal to decadal scales, was added to the secular trend provided by Cayan to produce a 100-year projection of hourly water levels at the Presidio. This use of historical short-term variability (defined here as any variability other than the long-term trend) to represent future short-term variability requires two assumptions—first, that the probability distribution of short-term variability will remain unchanged under the climate change projections, and second, that these short-term variations and the secular component of the water-level time series at the Presidio site are linearly superposable. Cayan and others (2008) found the first of these assumptions to be true. The second follows as a reasonable approximation from the fact that the amplitude of both components—O(1 m)—is considerably smaller than the average depth near the Presidio site—O(100 m). This is because in sufficiently deep water, surface waves do not interact with the bottom and are thus unaffected by relatively small changes in mean depth.

With the first of the two required TRIM-2D input time series thus obtained, the Port Chicago time series was next produced. Lacking more than a few decades of data at the Port Chicago site, the approach used for the Presidio site was unworkable. The chosen solution was to map the Presidio time series to Port Chicago using a temporal version of the technique of constructed analogues (Hidalgo and others 2008). In this approach, the historical water-level time series

6

(1996–2007) at the two stations were used to create a "map" which generates a 100-year hourly water-level projection at Port Chicago based on the Presidio projection described above. Specifically, the Presidio projection was stepped through five days at a time, with the preceding and succeeding days included to make a week of data. Each of these seven-day periods was expressed as a linear combination of the 22 best-matching (using RMS error) seven-day periods from the historical Presidio record (22 was found to be the optimal number of matches). The same coefficients in this optimal linear combination were then applied to the corresponding seven-day periods from the historical Port Chicago record to produce the estimate of Port Chicago water levels for the corresponding projected five-day period, after dropping the first and last days (which were included to minimize boundary effects in the procedure). One constraint on the method is that matching weeks were restricted to the same quarter of the year as the target week, allowing some accounting of the influence of the annual cycle of storm surges and freshwater flow.

Stepping through the 100-year Presidio projection in this manner, a corresponding 100-year projection of hourly water levels was developed for the Port Chicago station. The described procedure was applied to the non-secular component of the Presidio projection, and the Rahmstorf secular trend was then added to the resulting Port Chicago time series. A more complete description of the original method (as applied to spatial fields instead of time series) is given in Hidalgo and others (2008).

Projecting future Port Chicago water levels based on historical water levels assumes that amplitudes are unchanged as mean depth increases. Recent test runs using a Delft3D model of the bay-delta (van der Wegen, personal communication) suggest that increasing mean sea levels would result in increased tidal amplitudes at Port Chicago, meaning the results presented here are conservative, particularly in the landward reach of the estuary. These same test runs also indicate that any attenuation between the Presidio and Port Chicago sites of the long-term sea level rise signal would be negligible, justifying the method described above.

A validation run of the above procedure was performed, in which a portion of the historical Presidio record (1996–2007) was mapped to Port Chicago, with the procedure modified to exclude the target week from being selected as one of the matching patterns. The resulting "mapped" Port Chicago time series agreed well with the actual observed time series, with an RMS error of 6 cm (compared to an average daily tidal range of 148 cm) and a correlation coefficient of $r > 0.99$.

Both the Presidio and the Port Chicago 100-year hourly projections were interpolated from an hourly to a six-minute time step, and a week of hindcast astronomical tides were prepended to allow for model spin-up. A run of TRIM-2D was performed using these inputs (with a real-world run time of three weeks), resulting in a 100-year projection of six-minute gridded water heights throughout San Francisco Bay corresponding to a sea level rise of 139 cm by 2100.

ANALYSIS

Based on the projections of gridded water-level time series, water-height fields were developed corresponding to combinations of (1) specific amounts of sea level rise, and (2) specific return intervals (for example, 100-year high water with 50-cm sea level rise). This was accomplished by first separating the water-level time series of each model grid cell into a long-term trend and a detrended short-term variability time series. The long-term trend was estimated as the optimal second-degree least-squares fit to the full time series, and the residual was the short-term variability. Using the parameters of the long-term fits, the bay-wide, mean water-height field that corresponds to a specific amount of sea level rise could then be determined, providing (1) above. These fits to the long-term trends were sufficiently robust that for the subsequent analysis, it was decided they could reasonably be extended a few years beyond the end of the fitted data to represent a sea level rise of 150 cm, which would have occurred in an extended CCSM3-A2 scenario in 2105.

Return intervals represent the average period between events of a certain magnitude (corresponding to

"return levels"), such as floods, and are widely used for a variety of purposes, such as design and planning, regulation, and insurance requirements. High-water levels corresponding to specific return intervals associated with short-term variability were calculated next using the detrended 100-year time series at each grid cell. For periods less than a year, these series were long enough that water-level extremes could be robustly calculated simply as the corresponding mean. Mean daily higher-high water (MHHW) levels and mean daily lower-low water (MLLW) levels were calculated in this manner.

Return intervals of one year and longer were evaluated by applying the generalized extreme value (GEV) distribution, formulated by Fisher and Tippett (1928). Fisher and Tippett showed that block maxima, or a series of maxima each calculated over a specific time interval (for example, annual high-water levels), are characterized by the cumulative distribution function given in Equation 1.

Equation 1

$$F(x;\mu,\sigma,\xi) = \begin{cases} exp\left\{-[1+\xi(\frac{x-\mu}{\sigma})]^{-\frac{1}{\xi}}\right\}, & 1+\xi(\frac{x-\mu}{\sigma})>0 \\ exp\left\{-exp[-(\frac{x-\mu}{\sigma})]\right\}, & \xi=0 \end{cases}$$

The cumulative distribution function of Equation 1 was fit to the annual maxima of the detrended time series in each grid cell throughout the bay using the maximum-likelihood method[1], also developed by Fisher (1922). This resulted in values of the parameters μ, σ, and ξ for each grid cell. The most important of these parameters, ξ, is called the shape parameter and determines the shape of the extreme tail of the probability distribution of the process being characterized—in this case water-level variability. For all points on the bay grid, ξ < 0, representing a short-tailed process. This indicates relatively small differences between high-water levels for progressively longer return intervals. The inverse of Equation 1 was

---

[1] All analysis and figures were produced using GRASS/QGIS, Matlab, and R statistical analysis software.

then used to determine water-level heights throughout the bay for a given return interval, corresponding to a specific value of the cumulative distribution function.

Finally, for a specified amount of sea level rise we can determine the gridded mean water level throughout the bay using the parameters describing the long-term trend. For a specified return interval we can determine the associated water-height field using the GEV parameters, or, in the case of tidal time scales, using the corresponding mean high water or mean low water values. Adding the projected mean water levels to those characterizing short-term events allows the water-level extremes of the bay to be characterized, both probabilistically and through time for any combination of sea level rise and return interval.

This approach assumes that the simulated 100-year, water-level time series can be separated into a long-term trend and short-term variability with the latter component being stationary (a requirement of the GEV analysis), thus extending to the entire bay the assumption that the short-term variability is independent of the long-term trend. While this assumption was clearly reasonable near the deeper waters of the Presidio site, it is not obviously so in the shallower parts of the bay where surface waves may interact with the bottom. To test this assumption, a separate hydrodynamic simulation was carried out in which the long-term sea level trend was removed from the boundary conditions, leaving only the short-term component. The last few years of the 100-year projection were simulated in this manner, and the results were compared to the detrended signal derived from the output of the original simulation. If short-term variability is indeed independent of the long-term trend in mean sea level, the two should be identical. The test run showed very slightly higher peak water levels—O(1 cm)—only in the shoals of the bay, indicating that short-term variability in those near-shore areas is dampened negligibly by the increase in mean depth with sea level rise, justifying the approach used here.

Importantly, a benefit of this approach is that the results are not limited to the particular climate scenario used (in this case, CCSM3-A2). That is, the

results are not dependent on time elapsed in the scenario but instead on the specific amount of sea level rise that has occurred. By specifying this amount along with the statistics of the short-term variability (which, being stationary through time and across scenarios, are independent of the scenario chosen), the results are completely specified. Choosing a high-end scenario for the base simulation made it possible to parameterize and subsequently evaluate a large range of potential future sea level rise.

Using the approach described above, water-level extremes were determined for different values of sea level rise and return interval for each of the nearly 50,000 points in the TRIM-2D, 200-m horizontal grid. In particular, sea level rise was evaluated in half-meter increments: 0, 50, 100, and 150 cm. In Rahmstorf's projections (2007), these amounts of sea level rise would be reached in roughly the following time frames, respectively: present-day, 2050–2100, 2080–, and 2105– (the projections do not extend far enough into the future to provide end dates for the highest two values). For each of these four cases, the inverse of Equation 1 was used to determine the water-height fields corresponding to return intervals of 1, 10, 50, 100, and 500 years. Water-height fields for the tidal datums MLLW and MHHW were also determined for the four sea level rise values. Multiple intermediate amounts of sea level rise were also evaluated, but most results presented below focus on the half-meter increments.

Finally, each water-height field was compared at all points along the bay's shoreline to the adjacent land surface elevation data to assess what areas would be inundated (at least as often as the specified return interval, on average) by water at these heights, resulting in the inundation maps and data presented in the next section. A final data set used to portray vulnerable areas in terms of land cover type was the National Land Cover Data set of 2001 (NLCD01; Homer and others 2007).

Potential sources of error in this analysis include the source elevation data, particularly errors in adjusting the LiDAR data for dense vegetation to achieve "bare earth" elevations. As mentioned earlier, the effect of present or future levees, potential accumulation of

sediment and organic matter, and shoreline erosion are not included in this study. Further, attenuation of short-term variability over inundated areas has not been accounted for; therefore, vulnerability to inundation may be overstated for areas well removed from the bay's (and the TRIM-2D model's) present-day shoreline. The estimates presented in this study have not taken into account the effect of wind waves on water levels, nor, in the long term, the possibility of tsunamis. The effect of high freshwater inflows on stage are accounted for, but only corresponding to historical climate; increased winter flood peaks associated with climate warming (for example, Knowles and Cayan 2002) would likely produce greater inundation vulnerabilities than presented here, especially in the northern part of the estuary.

Finally, subsidence of the land surface may exacerbate some of the vulnerabilities presented here; conversely, long-term uplift may do the opposite. Bürgmann and others (2006) used IfSAR data to determine that recent magnitudes of tectonic vertical deformation have been small in the bay region (<0.5 mm/yr along the bay shoreline). Changes in groundwater levels in the Santa Clara Valley caused isolated subsidence near the southern tip of the bay of up to 30 mm/yr during the last century (Poland and Ireland 1988), though improved groundwater management has led to a more stable land surface there more recently (Galloway and others 1999; Schmidt and Bürgmann 2003).

A more widespread process is the ongoing consolidation of sediments and bay mud in filled areas adjacent to the bay, resulting in subsidence of up to 17 mm/yr (Ferretti and others 2004). Also, consolidation and compaction of organic sediments is common in managed wetlands. This is particularly evident in the Suisun marsh LiDAR data in the North Bay, although ongoing subsidence rates there are not well documented. These last two processes suggest that the results presented here are likely to underestimate the possible impacts of sea level rise, as wetlands and man-made fill dominate the low lying areas around the bay.

RESULTS AND DISCUSSION

Potential Inundation Due to Extreme High-water Levels

Extreme high-water levels pose the most serious threat of overtopping or breaching levees, which would cause flooding in currently protected areas. Under sea level rise, the threat to such areas would increase. Also, low-lying areas not currently vulnerable (and therefore not yet protected by levees) would become increasingly subject to inundation. Sea level rise would bring qualitatively different types of risks for wetlands, so they are excluded from the results in this section and are discussed in the next section.

Figure 5A shows areas whose elevations are below the adjacent average 100-year high-water levels under conditions of present mean sea level in blue, and under conditions of a (high-end) 150-cm increase in mean sea level in red. For clarity, intermediate values of sea level rise are not shown in this and subsequent maps; for smaller values of sea level rise, the red areas would be smaller. An interactive, high-resolution presentation of these results, with 50-cm increments individually color-coded, is available at *http://cascade.wr.usgs.gov/data/Task2b-SFBay*.

To better understand what types of land are at risk, Figure 5B shows the areas vulnerable to 100-year
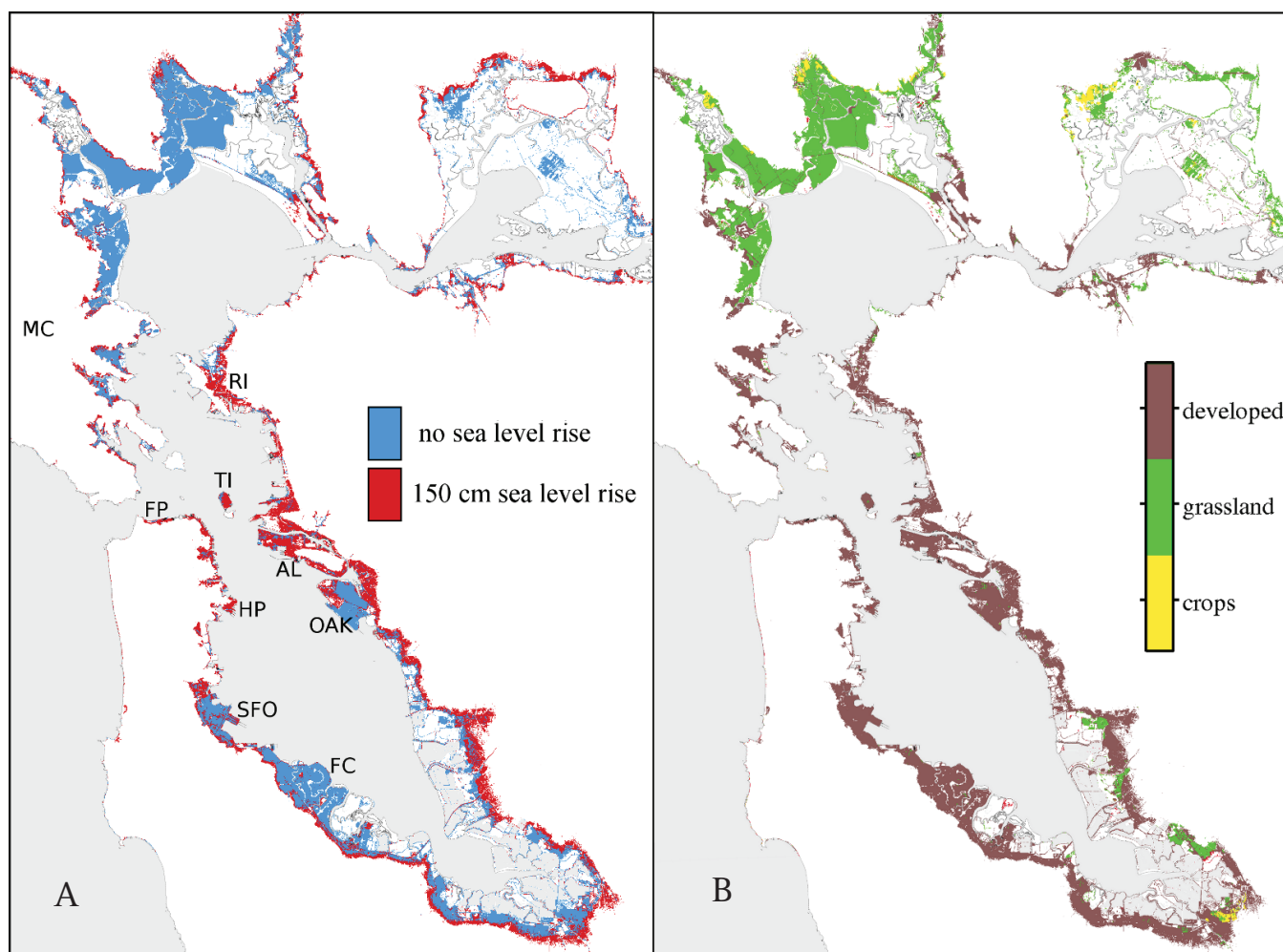
Figure 5 (A) Areas inundated or vulnerable to inundation under 100-year high-water levels for present-day (blue) and 150-cm sea level rise (red). MC=Marin County, RI=Richmond, TI=Treasure Island, FP=Fort Point, AL=Alameda, HP=Hunters Point, OAK=Oakland International Airport, SFO=San Francisco International Airport, and FC=Foster City. **(B)** Same areas as in (A), but colored according to land-use type. Wetlands are excluded from these figures.

inundation, expressed in terms of land cover types based on the NLCD01 data set.

Most of the areas indicated as presently vulnerable to inundation in Figure 5A (in blue) are behind levees and would only be inundated if those levees breached or were overtopped. These areas include crops and grasslands (mostly grazed pasture) that are primarily in North Bay, San Francisco and Oakland International Airports, and developed areas based on man-made fill, such as Foster City in South Bay. A primary concern is that with sea level rise, pressure on existing levees, and thus the risk of breaches, would be greatly increased. The potential for levee overtopping would also increase. In all these locations, existing levees would need to be raised and fortified to reduce the risk of these outcomes.

Other key areas of concern evident from Figure 5 include the municipal and industrial areas that are not currently vulnerable to 100-year high-water levels but would be under this future scenario. These areas (in red) run from Hunters Point to Fort Point in San Francisco, and include portions of eastern Marin, the Richmond peninsula, much of the East Bay shoreline including the former Naval Air Station at Alameda, and virtually all of Treasure Island. These are developed areas that would require some new levees and additions to any existing protection if flooding is to be prevented.

This ring of developed areas that would be newly vulnerable to inundation extends to South Bay, here falling upland of wetlands (existing or in restoration) and in some cases, upland of other (already vulnerable) developed areas. Many of these areas are already behind levees; they simply represent lands that are not currently at risk if these levees breached but would be at risk under the future scenario. Nearly all municipalities adjacent to South Bay (or adjacent to wetlands adjacent to South Bay) would face this risk to some degree, and again, existing protection would need to be improved. Another important concern for developed areas here is the survival of existing and future restored wetlands (the South Bay Salt Pond Restoration Project), which will depend on the ability of these wetlands to accrete material quickly enough to keep pace with sea level rise (wetlands are

discussed more in the next section). If the wetlands of South Bay were submerged by rising water levels, one consequence would be that wave energy would be less attenuated and erosional forces against protective upland levees would increase.

Figure 6 quantifies the different types of land at risk for a range of sea level rise amounts in terms of total vulnerable area in each land-use category. Excluding wetlands, the dominant categories of land cover around San Francisco Bay are grasslands and developed areas. The total area of vulnerable grassland would change little with sea level rise. Most *newly* vulnerable areas as a result of sea level rise would be the developed areas surrounding Central and South bays (see Figure 5). These also constitute the vulnerable areas with the greatest potential economic loss.

Excluding wetlands, today, a total area of about 310 km^2 is inundated or vulnerable to inundation under 100-year high-water levels; this consists almost entirely of grasslands and developed areas already protected by levees. Under a 50-cm sea level rise (projected by 2053 in the CCSM3-A2 scenario), the total vulnerable area would increase by 20% to 372 km^2, and under a 150-cm sea level rise (2105), the total vulnerable area would increase by almost 60% to 495 km^2. The largest change in area of a vulnerable land cover type would occur for developed areas. Vulnerable developed area would nearly double with a 150-cm sea level rise, from 157 km^2 to 311 km^2. These estimates assume no change in land-use assign-
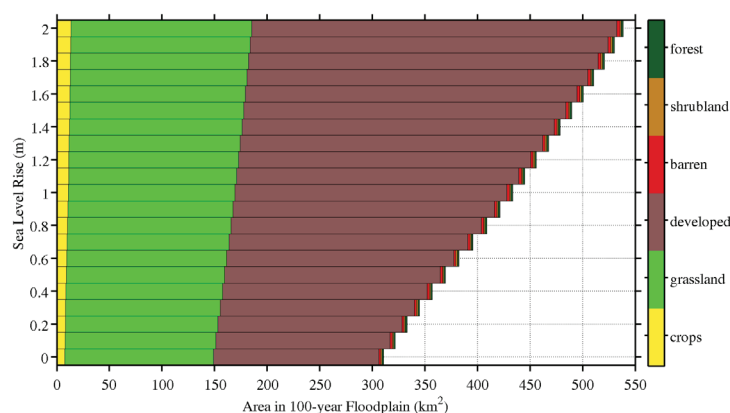
Figure 6 Total area around San Francisco Bay, excluding wetlands, vulnerable to inundation by 100-year high-water levels for a range of sea level rise, broken down into land-cover categories

ments over time; it is possible that some of the land currently assigned to other categories will ultimately be developed, resulting in an even greater value for total vulnerable developed area.

Figure 7 shows the bay-wide mean high-water levels and total area vulnerable to inundation for four values of sea level rise (0, 50, 100 and 150 cm) and five different return intervals (1, 10, 50, 100 and 500 years). As described earlier, water-level variability in the bay is a short-tailed process ($\xi < 0$), evidenced here by the progressively flatter response of water level and vulnerable area with increasing return interval. It should be noted that the 500-year return levels should include the effects of a potential tsunami, but the evaluation of such effects is beyond the scope of this investigation. Inclusion of tsunami effects would increase the 500-year return levels substantially. Under the high-end scenario of Rahmstorf (2007) (to which the CCSM3-A2 projection corresponds), the one-year peak event would nearly equal today's 100-year peak event by mid-century. This would not occur until 2100 under the low-end scenario (~50-cm sea level rise in 2100).

Wetlands and Changing Tidal Datums

There are about 400 km^2 designated in the NLCD01 as wetlands around San Francisco Bay, including the South Bay Salt Ponds, Napa Wetlands, and Suisun Marsh, among others. Figure 8 shows the amount of total wetland area, according to present-day wetland elevations, that would lie below projected future tidal datums as sea level rise progresses.

Some of the wetland area that appears as currently near the lower end of the tidal range consists of managed wetlands behind levees and other control structures. In those cases, sea level rise would threaten levee integrity and the ability to manage the wetlands for their desired uses. Wetlands not behind levees would gradually shift lower in the tidal range if elevations were to remain at their present levels. A 110-cm sea level rise would more than double the area of wetlands below local mean sea level (LMSL).

Figure 9 illustrates the spatial pattern of this shift, relative to MLLW, for the Napa and Suisun wetlands.
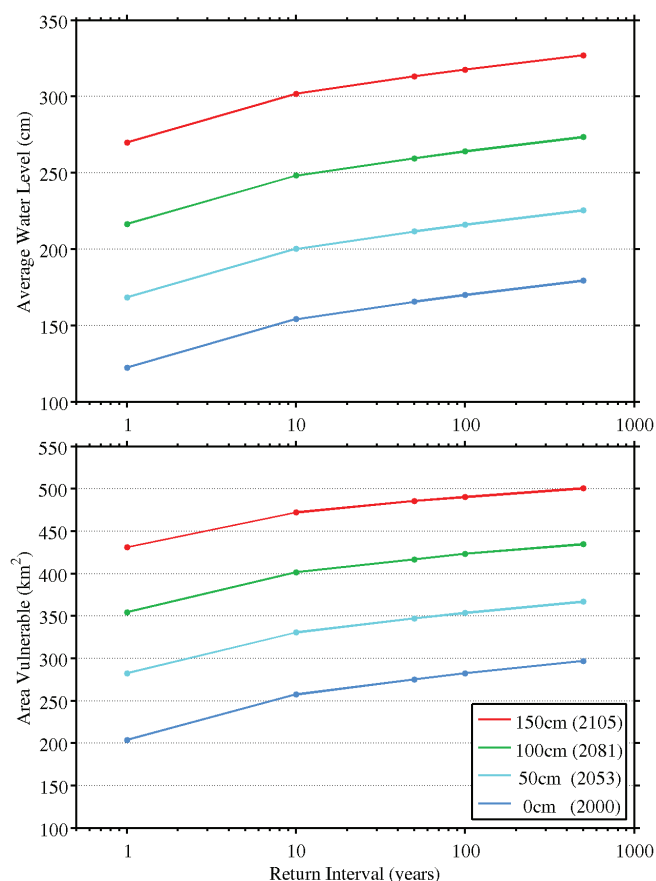
Figure 7 Bay-average water level relative to mean sea level (upper) and total area around San Francisco Bay, excluding wetlands, vulnerable to inundation (lower) versus return interval for four values of sea level rise. The earliest year in which each level is projected to be reached (using the high-end CCSM3-A2 projection) is indicated in the legend. Low-end projections do not produce a 50-cm sea level rise until around 2100.

Portions of Suisun Marsh are already subtidal. Under a 100-cm sea level rise, most of today's Suisun Marsh would be in the subtidal zone. With a 150-cm sea level rise, Napa Wetlands would be as well. Similar results are obtained for the South Bay Salt Ponds (not shown).

It is very important to note that Figures 8 and 9 ignore the dynamic nature of wetlands, particularly their ability to accrete organic and mineral sediment. The purpose here is to illustrate the magnitude of the potential changes which these processes would need to counter.
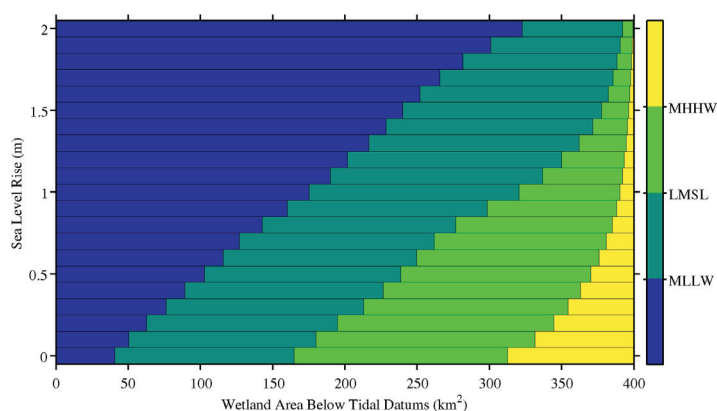
Figure 8 Total wetland area relative to fields of mean daily higher-high water levels (MHHW), local mean sea level (LMSL), and mean daily lower-low water levels (MLLW). These results are based on present-day elevations and ignore the potential for vertical accretion and lateral migration of wetlands in response to sea level rise.

The results of this study indicate that, to maintain their current positions in the tidal range, existing wetlands around San Francisco Bay would require 150, 330, or 530 million cubic meters (Mm^3) of (organic plus mineral) sediment[2] for respective sea level rise amounts of 50, 100, and 150 cm. Because sea-level projections over the coming century are generally quadratic in time, as typified by Figure 3, the *rate* of rise would increase linearly, starting at the present-day value of 20 to 30 mm/yr. The "break-even" sediment accumulation rate would also increase linearly, starting at the corresponding value of roughly 0.6 Mm^3/yr. Recent projections suggest that sea level could rise as little as 50 cm, or as much as 150 cm, by 2100. In the first case, the required accumulation rate would increase to 2.4 Mm^3/yr by 2100 (corresponding to a sea level rise rate of 6.7 mm/yr), averaging 1.5 Mm^3/yr over the century. In the second, the required rate would reach 10.1 Mm^3/yr by 2100 (25.6 mm/yr), averaging 5.3 Mm^3/yr. If leveed wetlands remained isolated from sediment supplies despite higher sea levels, these sediment volumes would be smaller. However, those levees would require substantial

---

2 These are estimates of the volume of accretion that would be required to maintain the vertical position within the tidal range of wetland areas already below MHHW, and to keep elevations of the remaining wetland areas just above MHHW. These values ignore depth increases in most mudflats, in subtidal shallow water habitat, and in wetland areas lacking elevation data due to the presence of open water at the time of data acquisition.

improvements to hold, and some common management practices, such as seasonal gravity draining of leveed wetlands managed as waterfowl habitat, would eventually become impossible in the absence of significant accretion.
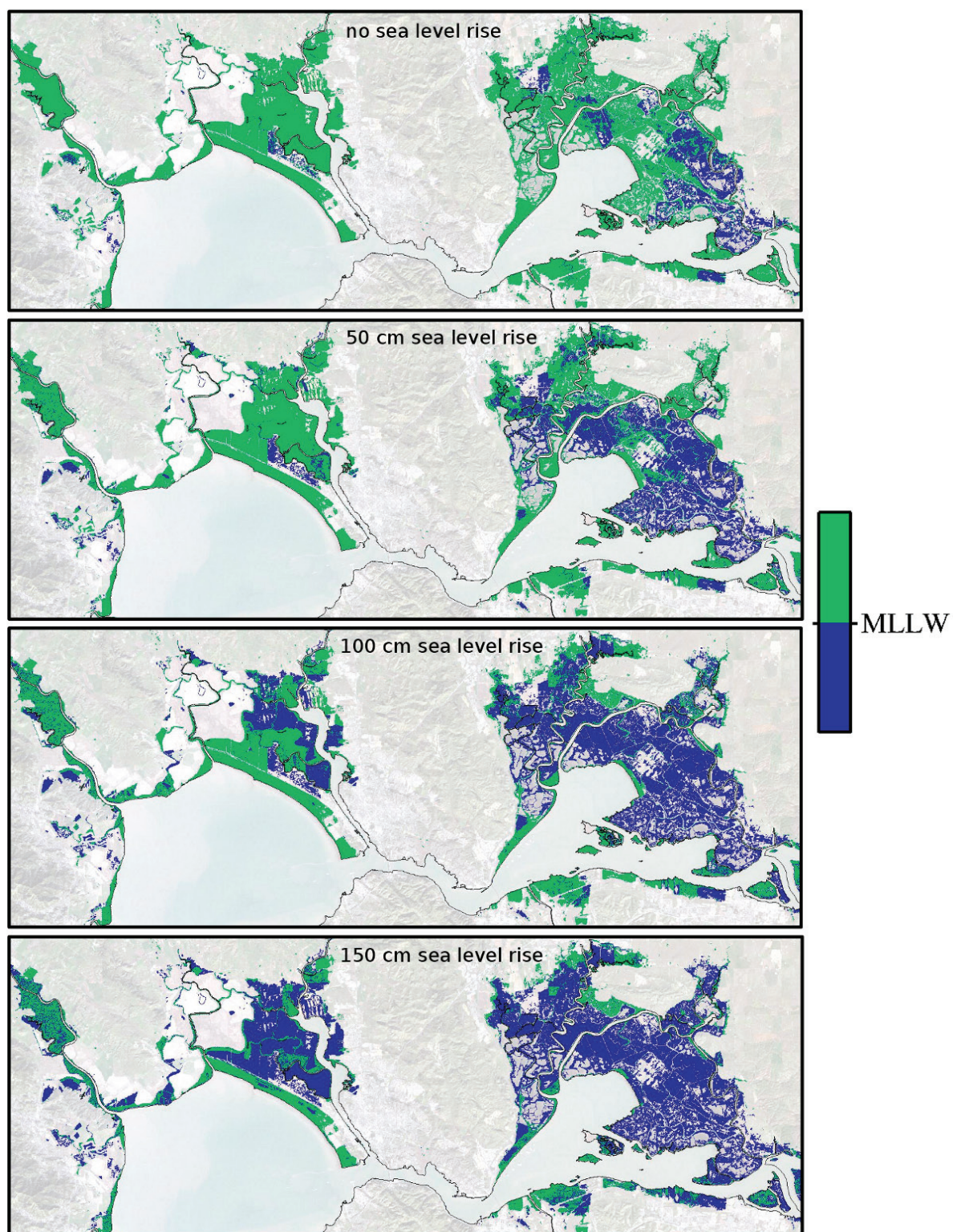
To give the above sediment flux values some context– in recent years, inorganic sediment input to the bay from the delta and local tributaries has averaged roughly 1.9×10^6 Mg/yr (Schoellhamer and others 2005; McKee and others 2006), though there is evidence that the delta portion of this supply has been in decline (Wright and Schoellhamer 2004). Depending on the density estimate used (D. Schoellhamer, personal communication), this amounts to roughly 1.5 to 3.8 Mm^3/yr, of which only about 10% has been depositing on wetlands (Schoellhamer 2005).

Wetland deposition rates are likely to increase as presently leveed wetlands become tidally connected through restoration actions (Schoellhamer 2005) and possibly as a result of levee breaches induced by sea level rise. Nonetheless, Ganju and Schoellhamer (2010) show that even under an extremely modest rate of sea level rise, present-day inorganic sediment supply may not suffice to keep the shallowest areas of Suisun Bay from getting deeper, which may have similar implications for the adjacent wetlands.

Although the topic of sustainable wetland restoration is complex (for example, Orr and others 2003) and beyond the scope of this study, it is worth noting here some other important factors that could contribute to wetland survival in the context of rising sea levels. For instance, dredged material from the bay may come to play a greater role in augmenting wetland elevations (Johnck and others 2009). Also, Drexler and others (2009) found that in tidal freshwater marshes in the delta, vertical accretion of peat ranged from 0.3 to 4.9 mm/yr over the past 6,000 years, indicating that given suitable conditions, peat formation can play an important role in mitigating the effects of sea level rise. There is even evidence that, at least in some parts of the bay, wetlands are capable of keeping pace with even higher rates of relative sea level rise than have been discussed here. In far South Bay, rates of sedimentation and organic accumulation were sufficient to allow salt marshes

Figure 9 Wetland elevations relative to the MLLW tidal datum for four values of sea level rise. Napa wetlands are left-of-center, and Suisun Marsh is on the right. These results are based on present-day elevations and ignore the potential for vertical accretion and lateral migration of wetlands in response to sea level rise.

to compensate for an estimated one meter of subsidence due to groundwater extraction over only a few decades (Patrick and DeLaune 1990; Watson 2004). However, far South Bay has been shown to be a particularly strong depositional environment relative to other areas of San Francisco Bay (Foxgrover and others 2004; Jaffe and Foxgrover 2006). Another wetland survival mechanism not discussed above is migration to adjacent upland areas. Though this possibility is generally limited in the highly developed bay region, some promising candidate areas exist (Enright and others 2007).

CONCLUSIONS

The main features of inundation around San Francisco Bay associated with potential sea level rise have been presented here. Results for several different values of sea level rise were given, and it should be re-emphasized that these results apply regardless of when a given amount of sea level rise is reached. Some major concerns associated with sea level rise were discussed—survival of existing wetlands, inundation of currently unprotected developed areas, increased risk of failure and overtopping of existing levees, and increased consequences of such failures as more areas become vulnerable are all real dangers. However, many other complications could also occur. For example, sanitation districts around the estuary are concerned that as sea level rises, seawater could backflow into their drainage systems, causing local flooding and sanitation problems. The risks of such problems occurring will increase gradually with sea level rise, but are associated with specific events within a given year. The largest events are most likely to occur during winter storms, particularly those coinciding with a spring tide. El Niño events also lead to higher water levels and increased risk (Cayan and others 2008).

The projected changes have many implications for those living in this region. Municipal planners will need to carefully consider the increasing risks of development in low-lying areas. Changing recurrence levels will require that flood insurance maps be redrawn regularly. Local groundwater pumping will need to continue to be carefully managed to avoid

subsidence. Transportation infrastructure will be threatened. Economic and policy implications of these and other changes are discussed in reports, based in part on the results presented here, by Heberger and others (2008) and BCDC (2009).

As mentioned in the "Data and Methods" section, these results can be applied to a wide range of climate change scenarios. For example, scenarios representing higher greenhouse gas emissions in the future can result in projections of large warming and sea level rise. In such a high-end scenario, conditions in 2100 may most closely resemble the results presented here for the 150-cm sea level rise amount. Conversely, estimates of sea level rise under the most optimistic of scenarios, representing lower greenhouse gas emissions, range from 45 to 70 cm by 2100 (Moser and others 2008). In this case, the 50-cm scenario may correspond to conditions in 2100. In terms of a specific result, referring to Figure 7, this means that under the most optimistic scenario, in 2100 the 1-year peak event would nearly equal today's 100-year peak event.

It is important to note, however, that global CO_2 emissions in recent years have tracked the highest scenarios considered to date in the IPCC Assessments (TCD 2009), and the results corresponding to the high-end scenarios of sea level rise presented in this study should be seriously considered as future possibilities. Further, sea level rise is expected to continue well beyond this century. Vellinga and others (2008) estimate the high end of possible sea level rise by 2200 to be 1.5 to 3.5 m, and Schubert and others (2006) provide a mid-range estimate, corresponding to a 3°C warming, of 3 to 5 m by 2300.

Understanding and successfully adapting to these changes will require a fuller knowledge of the likely consequences and the types of actions required. An example of a gap in our current knowledge is the need for a better understanding of the adaptability of existing and restorable wetlands and the dependence of the survival of these wetlands on the bay's sediment budget. Another very important missing piece of information is a better characterization of levee heights and their recent changes due to subsidence or uplift, and an associated regional data base.

Inundation data layers from this project are publicly available at *http://cascade.wr.usgs.gov/data/Task2b-SFBay* in the hope that the high-resolution regional data produced for this analysis will be useful for other regional and local studies and planning efforts.

REFERENCES

BCDC. 2009. Proposed Bay Plan amendment 1-08 concerning climate change. Bay Conservation and Development Commission draft report. Available from: *http://www.bcdc.ca.gov/proposed_bay_plan/bp_amend_1-08.shtml*

Bindoff NL, Willebrand J, Artale V, Cazenave A, Gregory J, Gulev S, Hanawa K, Le Quere C, Levitus S, Nojiri Y, Shum CK, Talley LD, Unnikrishnan A. 2007. Observations: oceanic climate change and sea level. In: Solomon S, Qin D, Manning M, Chen Z, Marquis M, Averyt KB, Tignor M, Miller HL, editors. Climate change 2007: the physical science basis. Contribution of Working Group I to the 4th Assessment Report of the Intergovernmental Panel on Climate Change. Cambridge, UK: Cambridge University Press. Available from: *http://www.ipcc.ch/ipccreports/ar4-wg1.htm*

Bürgmann R, Hilley G, Ferretti A, Novali F. 2006. Resolving vertical tectonics in the San Francisco Bay area from GPS and permanent scatterer InSAR analysis. Geology 34:221–224.

Cayan DR, Bromirski PD, Hayhoe K, Tyree M, Dettinger MD, Flick RE. 2008. Climate change projections of sea level extremes along the California coast. Climatic Change 87 (Suppl 1):S57–S73.

Cayan DR, Tyree M, Dettinger MD, Hidalgo H, Das T. 2009. California climate change scenarios and sea level rise estimates for the California 2008 Climate Change Scenarios Assessment. California Energy Commission Report No. CEC-500-2009-014-F. Available from: *http://www.energy.ca.gov/2009publications/CEC-500-2009-014/CEC-500-2009-014-F.PDF*

Cheng RT, Casulli V, Gartner JW. 1993. Tidal, residual, intertidal mudflat (TRIM) model and its applications to San Francisco Bay, California. Estuarine, Coastal and Shelf Science 36:235–280.

Cheng RT, Gartner JW. 1984. Tides, tidal and residual currents in San Francisco Bay California - results of measurements, 1979–1980. U.S. Geological Survey Water-Resources Investigations Report No. 84-4339.

Church JA, White NJ, Coleman R, Lambeck K, Mitrovica JX. 2004. Estimates of the regional distribution of sea level rise over the 1950–2000 period. Journal of Climate 17:2609–2625.

Church JA, White NJ. 2006. A 20th century acceleration in global sea-level rise. Geophysical Research Letters 33:L01602.

Coons T, Soulard CE, Knowles N. 2008. High-resolution digital terrain models of the Sacramento-San Joaquin Delta region, California. U.S. Geological Survey, Data Series 359. Available from: *http://pubs.usgs.gov/ds/359*.

Drexler JZ, de Fontaine CS, Brown TA. 2009. Peat accretion histories during the past 6,000 years in marshes of the Sacramento-San Joaquin Delta, CA, USA. Estuaries and Coasts 32(5):871-892.

Enright C, Wang X, Dudas J. 2007. Elevation matters: wetland restoration where it wants to be [presentation]. Interagency Ecological Program 2007 Annual Workshop; 2007 Feb 28-Mar 2; Pacific Grove (CA). Available from: *http://www.water. ca.gov/suisun/dataReports/docs/IEP2007_LiDAR-WetlandRestoration.pdf*

Ferretti A, Novali F, Bürgmann R, Hilley G, Prati C. 2004. InSAR permanent scatterer analysis reveals ups and downs in the San Francisco Bay area. EOS (Transactions, American Geophysical Union) 85:317.

Fisher RA. 1922. On the mathematical foundations of theoretical statistics. Philosophical Transactions of the Royal Society of London, Series A 222:309–368.

Fisher RA, Tippett LHC. 1928. Limiting forms of the frequency distribution of the largest or smallest member of a sample. Proceedings of Cambridge Philosophical Society 24:180–190.

Flick R. 2003. Trends in United States tidal datum statistics and tide range. Journal of Waterway, Port, Coastal and Ocean Engineering 129(4):155–164.

Foxgrover AC, Higgins SA, Ingraca MK, Jaffe BE, and Smith RE. 2004. Deposition, erosion, and bathymetric change in South San Francisco Bay: 1858–1983. U.S. Geological Survey Open-File Report 2004-1192, 25 p. Available from: *http://pubs.usgs.gov/of/2004/1192*

Foxgrover AC, Jaffe BE. 2005. South San Francisco Bay 2004 topographic LiDAR survey: data overview and preliminary quality assessment. U.S. Geological Survey Open-File Report 2005–1284, 57 p. Available from: *http://pubs.usgs.gov/of/2005/1284*

Galloway DL, Jones DR, and Ingebritsen SE. 1999. Land subsidence in the United States. U.S. Geological Survey Circular 1182, 175 p. Available from: *http://pubs.usgs.gov/circ/circ1182*

Ganju NK, Schoellhamer DH. 2010. Decadal-timescale estuarine geomorphic change under future scenarios of climate and sediment supply. Estuaries and Coasts 33:15-29.

Gleick PH, Maurer EP. 1990. Assessing the costs of adapting to sea-level rise: a case study of San Francisco Bay. Pacific Institute Report. Available from: *http://www.pacinst.org/reports/sea_level_rise_ sfbay*

Heberger M, Cooley H, Herrera P, Gleick PH, Moore E. 2008. The impacts of sea-level rise on the California coast. California Energy Commission Report No. CEC-500-2009-024-F. Available from: *http://www.energy. ca.gov/2009publications/CEC-500-2009-024/CEC-500-2009-024-F.PDF*

Hidalgo H, Dettinger MD, Cayan DR. 2008. Downscaling with constructed analogues—Daily precipitation and temperature fields over the United States. California Energy Commission Report No. CEC-500-2007-123. Available from: *http://meteora. ucsd.edu/cap/pdffiles/analog_pier_report.pdf*

Homer C, Dewitz J, Fry J, Coan M, Hossain N, Larson C, Herold N, McKerrow A, VanDriel JN, Wickham J. 2007. Completion of the 2001 national land cover database for the conterminous United States. Photogrammetric Engineering and Remote Sensing 73:337-341. Available from: *http://www.epa.gov/ mrlc/nlcd-2001.html*

[IPCC] Intergovernmental Panel on Climate Change. 2001. Climate change 2001, the third assessment report (AR3) of the United Nations Intergovernmental Panel on Climate Change. Available from: *http:// www.ipcc.ch/publications_and_data/publications_ and_data_reports.htm*

[IPCC] Intergovernmental Panel on Climate Change. 2007. Climate Change 2007, the fourth assessment report (AR4) of the United Nations Intergovernmental Panel on Climate Change. Available from: *http:// www.ipcc.ch/publications_and_data/publications_ and_data_reports.htm*

Jaffe BE, Foxgrover AC. 2006. Sediment deposition and erosion in South San Francisco Bay, California from 1956 to 2005. U.S. Geological Survey Open-File Report 2006–1262, 24 pp. Available from: *http:// pubs.usgs.gov/of/2006/1287*

Johnck E, Collins J, Dingler J, Grossinger R, Kendall T, Ross B, Werme C. 2009. Dredged sediment: from "spoils" to valued resource. In: The pulse of the estuary: monitoring and managing water quality in the San Francisco Estuary. SFEI Contribution 583. San Francisco Estuary Institute, Oakland, CA. Available from: *http://www.sfei.org/rmp/pulse/2009*

Knowles N, Cayan D. 2002. Potential effects of global warming on the Sacramento-San Joaquin watershed and the San Francisco Estuary. Geophysical Research Letters 29:38-1–38-4. Available from: *http://tenaya. ucsd.edu/~knowles/papers/knowles_grl_2002.pdf*

McKee LJ, Ganju NK, Schoellhamer DH. 2006. Estimates of suspended sediment flux entering San Francisco Bay from the Sacramento and San Joaquin Delta, San Francisco Bay, California. Journal of Hydrology 323:335-352.

Mitasova H, Hofierka J. 1993. Interpolation by regularized spline with tension: II. Application to terrain modeling and surface geometry analysis. Mathematical Geology 25:657–667.

Moser SC, Cayan DR, Franco G. 2008. The Future Is Now—An Update on Climate Change Science, Impacts, and Response Options for California. California Climate Change Center CEC Report No. CEC-500-2008-071. Available from: *http://www. energy.ca.gov/2008publications/CEC-500-2008-071/ CEC-500-2008-071.PDF*

Orr M, Crooks S, Williams PB. 2003. Will Restored Tidal Marshes Be Sustainable? San Francisco Estuary and Watershed Science [Internet]. Available from: *http://escholarship.org/uc/item/8hj3d20t*

Patrick WH, Delaune RD. 1990. Subsidence, accretion, and sea level rise in South San Francisco Bay marshes. Limnology and Oceanography 35(6):1389–1395.

Pfeffer WT, Harper JT, O'Neel S. 2008. Kinematic constraints on glacier contributions to 21st-Century sea-level rise. Science 321(5894):1340–1343.

Poland JF, Ireland R.L. 1988. Land subsidence in the Santa Clara Valley, California, as of 1982, mechanics of aquifer systems, U.S. Geological Survey Professional Paper 497-F, 61 p. Available from: *http://pubs.er.usgs.gov/usgspubs/pp/pp497F*

Rahmstorf S. 2007. A semi-empirical approach to projecting future sea-level rise. Science 315:368–370.

Schmidt DA, Bürgmann R. 2003. Time-dependent land uplift and subsidence in the Santa Clara Valley, California, from a large InSAR data set. Journal of Geophysical Research 108:2416.

Schoellhamer DH, Lionberger MA, Jaffe BE, Ganju NK, Wright SA, Shellenbarger G. 2005. Bay sediment budget: sediment accounting 101. In: The pulse of the estuary: monitoring and managing water quality in the San Francisco Estuary. SFEI Contribution 411. San Francisco Estuary Institute, Oakland, CA. Available from: *http://www.sfei.org/rmp/pulse/2005*

Schubert R, Schellnhuber H-J, Buchmann N, Epiney A, Griebhammer R, Kulessa M, Messner D, Rahmstorf S, Schmid J. 2006. WBGU - German Advisory Council on Global Change: The Future Oceans - Warming Up, Rising High, Turning Sour. WBGU, Berlin. Available from: *http://www.wbgu.de/wbgu_ sn2006_en.pdf*

[TCD] The Copenhagen Diagnosis. 2009. Updating the world on the latest climate science. Allison I, Bindoff NL, Bindschadler RA, Cox PM, de Noblet N, England MH, Francis JE, Gruber N, Haywood AM, Karoly DJ, Kaser G, Le Quéré C, Lenton TM, Mann ME, McNeil BI, Pitman AJ, Rahmstorf S, Rignot E, Schellnhuber HJ, Schneider SH, Sherwood SC, Somerville RCJ, Steffen K, Steig EJ, Visbeck M, Weaver AJ. Sydney, Australia: The University of New South Wales Climate Change Research Centre (CCRC). 60 p. Available from: *http://www.copenhagendiagosis.org*

Vellinga P, Katsman C, Sterl A, Beersma J, Hazeleger W, Church J, Kopp R, Kroon D, Oppenheimer M, Plag H-P, Rahmstorf S, Lowe J, Ridley J, von Storch H, Vaughan D, van de Wal R, Weisse R, Kwadijk J, Lammersen R, Marinova N. 2008. Exploring high-end climate change scenarios for flood protection of the Netherlands: an international scientific assessment. Wageningen, the Netherlands: KNMI. Available from: *http://www.knmi.nl/bibliotheek/knmipubWR/WR2009-05.pdf*

Watson EB. 2004. Changing elevation, accretion, and tidal marsh plant assemblages in South San Francisco Bay tidal marsh. Estuaries 27(4):684–698.

Wigley TML. 2005. The climate change commitment. Science 307:1766–1769.

Williams PB. 1985. An overview of the impact of accelerated sea level rise on San Francisco Bay. Project No. 256 for the Bay Conservation and Development Commission. San Francisco, California: Philip Williams & Associates.

Williams PB. 1987. The impacts of climate change on the salinity of San Francisco Bay. EPA Report No. EPA-230-05-89-051. San Francisco, California: Philip Williams & Associates.

Wright SA, Schoellhamer DH. 2004. Trends in the sediment yield of the Sacramento River, California, 1957–2001. San Francisco Estuary and Watershed [Internet]. Available from: *http://escholarship.org/uc/item/891144f4*